

The Integration of the Morphological Aspects of Sand to It's Shear Strength and Dilatancy Characteristics.

Alvin John Lim Meng Siang¹, Devapriya Chitral Wijeyesekera², Adnan bin Zainorabidin³, Ismail bin Hj Bakar⁴

^{1,2,3,4}Faculty of Civil and Environmental Engineering, UTHM

Abstract: The integration of geological and morphological features to the geotechnical characteristics of coarse grain soils can lead via statistical methods to determined correlations between strength and its physical properties. The shape and sizes of sand particles reflect the formation history of the grains where it results from the disintegration of rocks due to water, weather and glaciers. The particle interactions of sand due to shear deformation and also seismic reactions of different shape and sizes would result in various sedimentological macroscale behaviour. Clean sands are cohesionless ($c = 0$) but have a finite friction angle (ϕ) and its shear strength is entirely dependent on the density, normal stress and interlocking particle structure. The latter is associated with the property of the angle of dilatancy (ψ) in particular with sands. Direct shear box testing was done on samples of well graded sand (SW) and poorly graded uniform sand (SPu_{Kahang}) from Kahang Malaysia and also (SPu_{L.Buzzard}) uniform Leighton Buzzard sand from the UK. The shapes of the sand particles were quantified using images obtained from a digital microscope. ϕ_{peak} , ϕ_{cr} and ψ are the highest for (SW) when compared with others. SPu_{L.Buzzard} sands showed a significant decrease in the values with similar relative density (D_r). High normal stresses give very little variations in the angle of dilatancy (ψ) between the samples tested as compared to the lower normal stress that was used. This research contributes to furthering the understanding of the engineering behaviour of sand and also helps in predicting the occurrence of dilation based on sand morphology in dynamic soil structure interaction.

Keywords: Sand, direct shear box test, friction angle, angle of dilatancy, size and shape.

1. Introduction

Coarse grained soils have unique sedimentological features where the wide range of shape and sizes of sand particles solicit further research into integration of geological principles and geotechnical aspects of the soil. The properties of sand largely depends on the rocks from which they are derived, however during its transportation by water prior to deposition the weaker particles tend to be selectively removed by attrition making the resulting material to become stronger aggregates than the parent rock when crushed [1].

The principal sources of sand are relatively young and unconsolidated superficial deposits which have accumulated in the geological past. These geological deposits include marine beach and lacustrine deposits, alluvial deposits, mountain slope solifluction wastes as well as those of the glacial deposits [2]. The combination of the nature of the sand particles and the weathering process of these deposits have caused different shapes and grading distribution to be formed respectively. The sedimentological characteristics of sand give unique engineering properties that make sand a good and necessary construction material in foundation engineering. However, extensive vibrations and shaking

due to seismic effect may lead to a phenomenon called liquefaction.

Previous studies have shown that subtle differences in proportions of different grain sizes and the organisation of these different deposits can produce significant differences in the particle morphodynamics [3]. Shear strength behaviour however has shown that the undrained residual strength decreases with the increase in the uniformity coefficient (C_u) and the average diameter (D_{50}) for a monotonic undrained triaxial test [4]. Cho et al. [5] in a the study of sphericity and roundness of crushed and natural sands observed using a stereomicroscope (Leica MZ6) on 30 different particles suggested that for large strain behaviour, the increase in irregularity causes an increase in the critical state friction angle (ϕ_{cr}). Rounded particles also show the undrained behaviour undergoes a schematic weakening where the shear stress undergoes reduction after a transient peak deviator stress for a torsional hollow cylinder test. Angular sand particles however show stable response with a continuous increase in strength after a transient peak [6].

In this present study, the relationship between shear strength parameter (ϕ_{peak} , ϕ_{cr}) and dilatancy (ψ) is investigated. Peak friction angle (ϕ_{peak}) is the parameter where a soil is in its peak strength. It may occur before or at critical state depending on the initials state of the soil

*Corresponding author: alvinjlims@gmail.com

being sheared. Critical friction angle (ϕ_{cr}) is the shearing strength at critical state, where the soil is in constant volume during shearing. In this state the grains being sheared have no significant granular interlock or sliding plane development affecting the resistance to shearing. In accordance with the explanation given by Budhu [7], the relationship between the shear strength of a soil using Coulombs frictional law and the dilatancy can be represented by equation 1, which shows the shear strength (τ) of a soil is a function of their dilatancy angle (ψ) and normal stress (σ_n).

$$\tau = \sigma_n \tan(\phi + \psi) \quad (1)$$

2. Materials Used for Testing

The test on sedimentological behaviour uses materials of river sands obtained from Kahang, Johor and also Leighton Buzzard sand (UK). Kahang sands comprised of two different particle size distribution classifications which are well graded sands (SW) and uniformly graded sands (SPu_{Kahang}). The raw or original sands from Kahang are generally classified as well graded sands. Careful

separation of the sand particles using sieves enabled uniformly graded sands to be obtained. Leighton Buzzard sand however, is documented as being uniformly graded sand and is referred to as (SPu_{L. Buzzard}). Classifications of the samples are in accordance with BS 1377-1: 1990 [8] and Head [9]. The angular shape of Kahang sands is compared with the more rounded Leighton Buzzard sands on its strength and dilatancy characteristics.

Figure 1 show the particle size distribution curves of all the samples illustrating the different grading curves. Table 1 is a factual summary of all the main properties of the samples in this study. The maximum void ratio (e_{max}) was obtained by using a measuring cylinder containing the sample and it was quickly turned upside-down to acquire a loose state (as specified in BS 1377-1: 1990). The minimum void ratios (e_{min}), were obtained by using a split mould and the sample was compacted by tamping and vibrating under water. Then a convenient stress was applied to the sample carefully avoiding particle crushing to obtain a dense state. Repeat tests done on the same sample gave variations not exceeding 0.005 for the minimum void ratio.

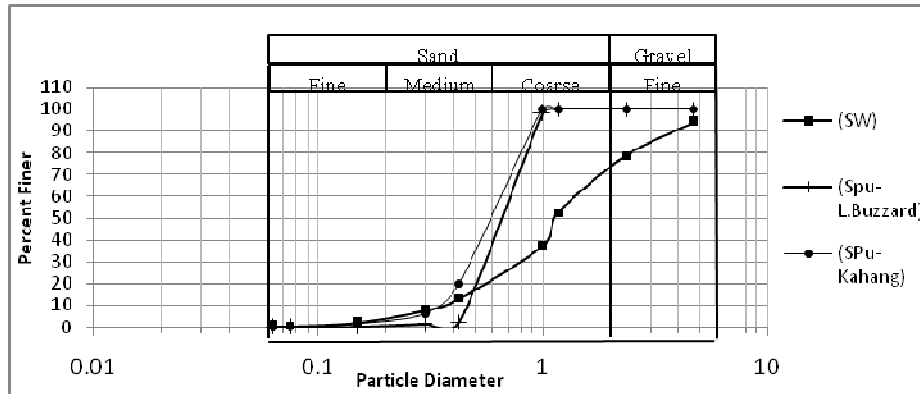


Figure 1: Particle size distribution curve

Table 1: Properties of the test samples

Type of sand	Gradation				Void Ratio	
	D ₆₀	D ₁₀	C _u	C _c	e _{max}	e _{min}
SW	1.5	0.38	3.95	1.10	0.914	0.398
SPu _{L. Buzzard}	0.71	0.48	1.48	0.95	0.725	0.574
SPu _{Kahang}	0.65	0.35	1.86	1.253	0.948	0.574

parameters are explained in Table 2 and the calculation is based on Figure 2.

3. The Quantification of the Shape of the Particles

The sedimentological characteristics of sand have shown that the genesis of sandy soils has resulted in different particle shapes to be formed. The quantification of the particle shapes is based on two important parameters which are its sphericity and roundness as stated by Cho et al [5]. The definition of these two shape

Table 2: Classification of shape parameters

Shape Parameter	Remarks	Equation
Sphericity (S)	The diameter of the largest inscribed sphere relative to the diameter of the smallest circumscribed sphere.	$S = \frac{r_{max-in}}{r_{min-cir}} \quad (2)$
Roundness (R)	The average radius of curvature of features relative to the radius of the maximum sphere that can be inscribed in the particle.	$R = \frac{\sum r_i / N}{r_{max-in}} \quad (3)$

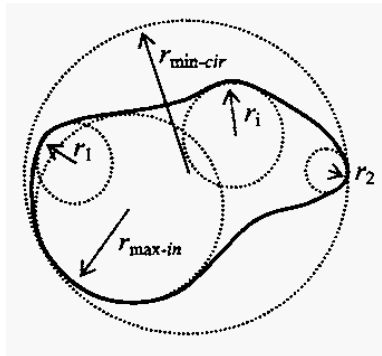


Figure 2: Quantification of the particle shape

Figure 3 represents the many shapes of sand particles which can be classified into its dimensionless parameters (Cho et al. [5], as quoted by Krumbein and Sloss, 1963). The regularity parameter is defined as the average of the two parameters with an attempt to unify the effect of roundness and sphericity as defined in equation (4). Thus the diagonal broken lines in Figure 3 correspond to constant particle regularity.

$$\rho = \frac{R + S}{2} \quad (4)$$

2

parameter values than that of the Kahang sand. Table 3 also shows that the mean sphericity and roundness of Leighton Buzzard sand are also higher than that of Kahang sand. Therefore, with reference to Figure 3, it is clear that these two types of sands have contrary shape parameters.

Shape comparisons are only made between the uniformly graded Kahang sands and the uniformly graded Leighton Buzzard sands, which have almost similar uniformity coefficients (C_u). A digital microscope as shown in Figure 4 was used to obtain micrographs of the sand particles shown in Figure 5. The digital microscope can take images with a magnification of up to (x500). A magnification image of x50 was sufficient for the quantification of the shape of the sand particles. In this research, fifty randomly picked sand particles of the two types of sand were analysed under the digital microscope and example calculations in obtaining the parameter are shown in Figure 6. Figures 7 and 8 give the analytical results and the extreme images respectively. The differences in the shape parameters are discussed.

The histogram in Figure 7 shows that the sphericity and roundness of each sample has a single mode distribution. The graphs show that Leighton Buzzard sand tends to have a mode distribution at higher shape

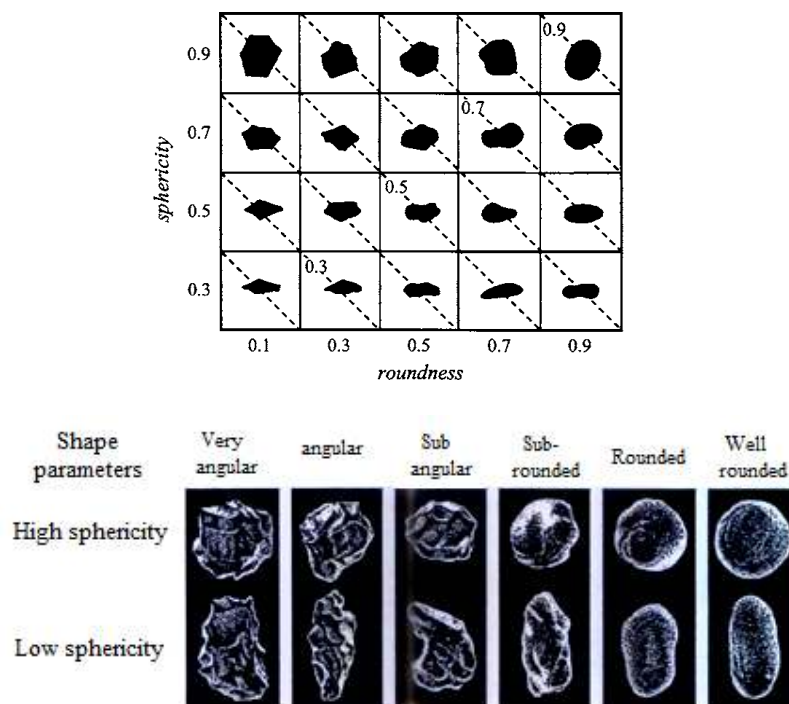


Figure 3: Particle shape determination (Cho et al, [5]; as presented in by Krumbein and Sloss, 1963, Tsomokos and Georgiannou [6])



Figure 4: a) Digital microscope used for analyzing particle shapes, b) Digital microscope software.

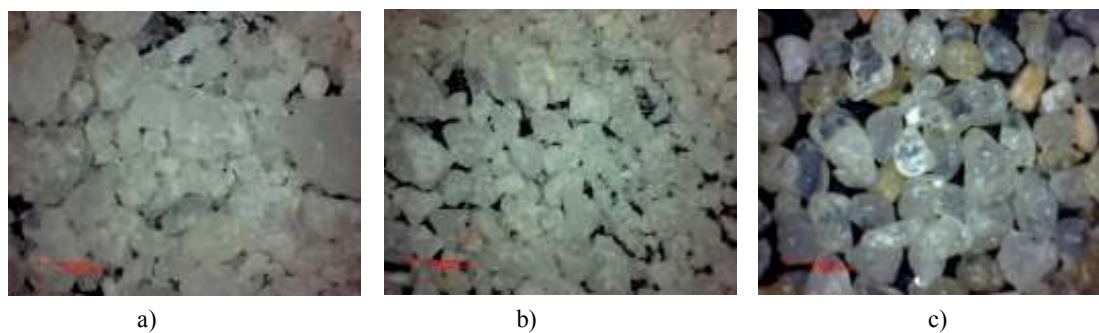


Figure 5: Magnified pictures of the sand particles (a) SW sand (b) SPu_{Kahang} sand (c) SPu_{L.Buzzard} sand.

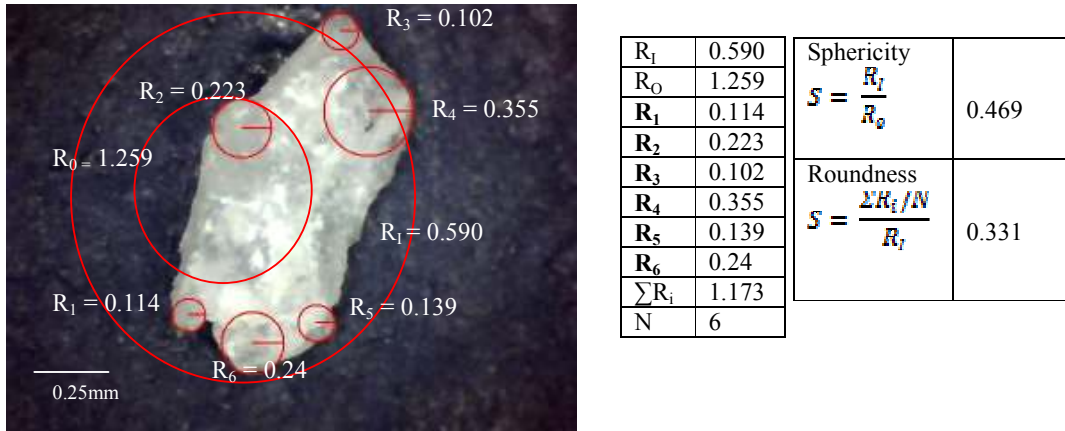


Figure 6: Example calculations in the determination of the shape parameters

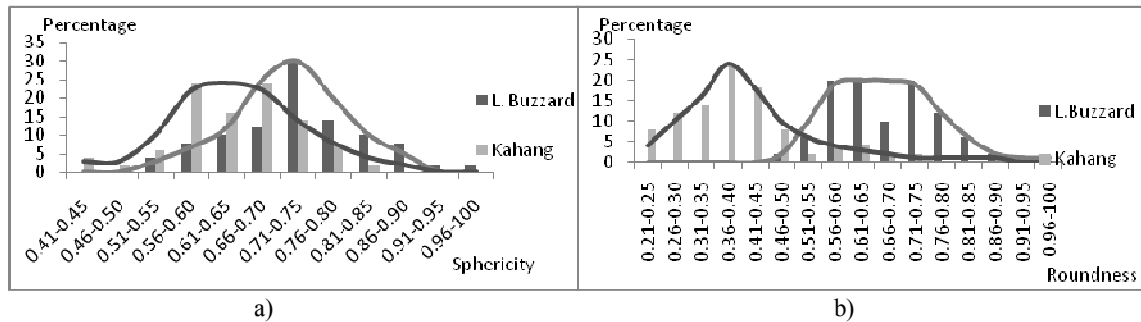


Figure 7: Percentage of (a) sphericity and (b) roundness of the particles

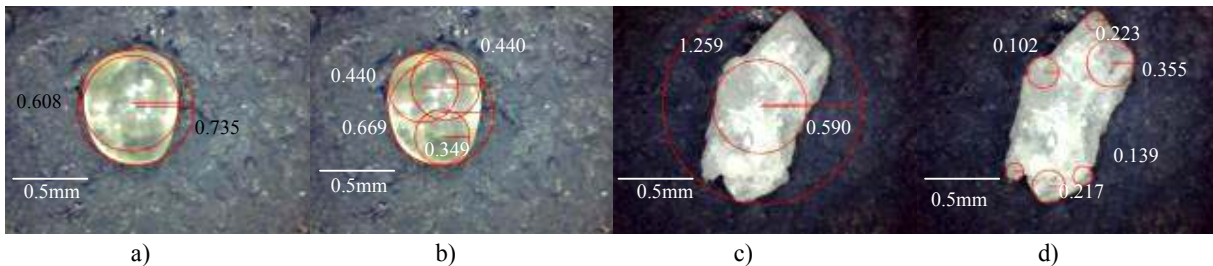


Figure 8: Images of extreme particles,

(a) & (b) SPu_{L.Buzzard} sand particle with Sphericity = 0.827 and Roundness = 0.78

(c) & (d) SPu_{Kahang} sand particle with Sphericity = 0.469 and Roundness = 0.325

Table 3: The range and average of the particle shapes

	Leighton Buzzard sand			Kahang sand		
	Sphericity	Roundness	Regularity	Sphericity	Roundness	Regularity
Minimum	0.52	0.46	0.57	0.45	0.23	0.39
Maximum	0.96	0.97	0.90	0.83	0.89	0.74
Mean	0.732	0.680	0.701	0.643	0.410	0.526
Mode	0.731	0.733	0.675	0.677	0.390	0.525
Std. Dev.	0.099	0.499	0.50	0.088	0.380	0.45

4. Direct Shear Box Test Result

Direct shear tests were done on natural dry samples, in a 60 x 60 x 20 mm shear box. Samples with different relative densities were prepared and each sample was

subjected to a normal stress (σ_n) of 25, 50 and 100 kPa. Bolton [10],[11] observed that particle crushing is not appreciable when the mean shear stress is lower than 150kPa, thus allowing dilation to be treated as a function of only the relative density below this stress. Particle crushing during shearing was avoided in this study by using the required low level normal stresses. Sieve analysis was done on the samples before and after the shear test where the particle size distribution curves show similar results. This proves as evidence that particle crushing was avoided.

Figure 9 shows typical results from direct shear box testing. It can be seen that the dilatancy angle coincide with the peak shear stress [12]. Figure 10(a) shows the direct shear testing of this research with a normal stress of 100kPa on well graded sand (SW) with different relative densities. Dense sand shows a peak shear stress (τ_{peak}) and then it levels out at a residual shear stress (τ_r), whereas loose sand structure only shows residual shear stress (τ_r). Figure 10(a) further shows that the residual shear stress (τ_r) for SW is almost the same for all the relative densities tested. This is a phenomenon of a soil mass that continuously deforms at constant volume, constant normal stress, constant shear stress and constant rate of shear strain [13]. It is therefore an important consideration in design and interpretation of shear results.

Figure 10(b) shows a negative vertical displacement, which means that the samples are in an expansion where

it increases in volume as shear displacement occur. This is called dilation, noticing that the sample with the lowest relative density doesn't show any dilation but it is however in compression at residual shear stresses. Bolton [10], Simoni and Houlsby [14], Hamidi et al [13] computed the angle of dilation (ψ) by relating the horizontal displacement (h) and vertical displacement (v) to calculate the rate of dilation (dv/dh) with the following equation:

$$\tan \psi = \frac{dv}{dh} \quad (5)$$

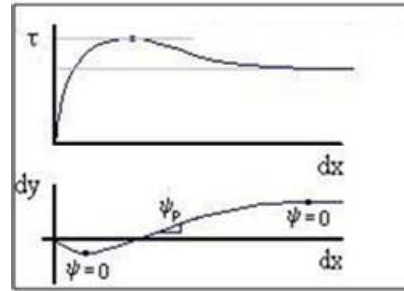


Figure 9: Typical direct shear results from direct shear box test [12]

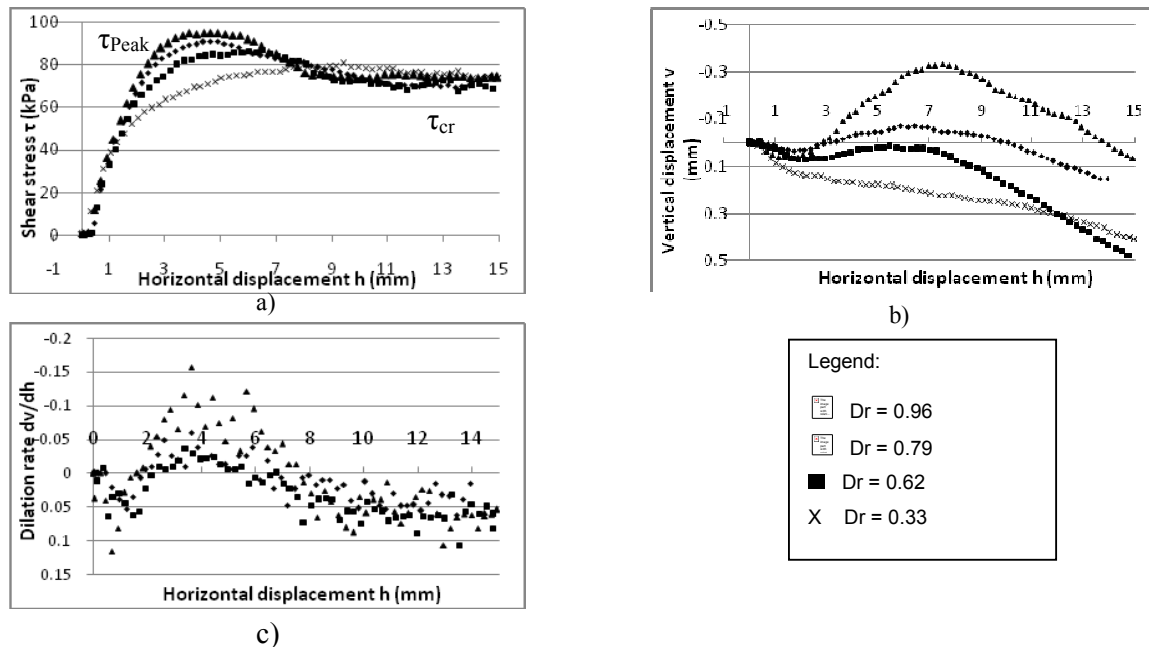


Figure 10: Typical direct shear test result of 100kPa normal stress of the, (a) shear stress (τ), (b) vertical displacement (mm), (c) dilation rate (dv/dh) versus horizontal displacement of well graded sand (SW) of various relative densities.

Figure 10(c) shows the variation of the rate of dilatancy with increasing horizontal shear displacement.

The dilatancy rate is calculated starting from zero horizontal displacement in the shear box. The increases in

horizontal displacement will affect the vertical displacement depending on the relative density of the sand. Any variation on the horizontal and vertical displacement helps to calculate the rate of dilatancy of the sample. As expected the maximum angle of dilation using equation 3, if found coincides with the peak value of the shear stress versus horizontal displacement graph. This enables the determination of the maximum angle of dilation ψ_{max} .

5. Shear Strength Characteristics of the Samples

Figure 11 shows the results of the peak friction angle (ϕ_{peak}) versus the relative density for all the samples with

different normal stress (σ_n). The peak friction angle is the lowest for $SPu_{(L.Buuzard)}$ sand. $SPu_{(Kahang)}$ also shows lower ϕ_{peak} than the SW sands but it is however higher than that of $SPu_{(L.Buuzard)}$. This indicates that the relative density, grading characteristics and the shape of the particles have a significant effect on the shear strength of the soil. The determination of critical friction angle (ϕ_{cr}) in this study is in line with the work of Simoni and Houlsby [14] and Hamidi et al. [13] where they use the ϕ_{peak} values of different densities plotted against maximum dilatancy angle (ψ_{max}) as shown in Figure 12. The best fit line is then drawn, giving the ϕ_{cr} values as the shearing resistance of a sample which would exhibit zero dilatancy.

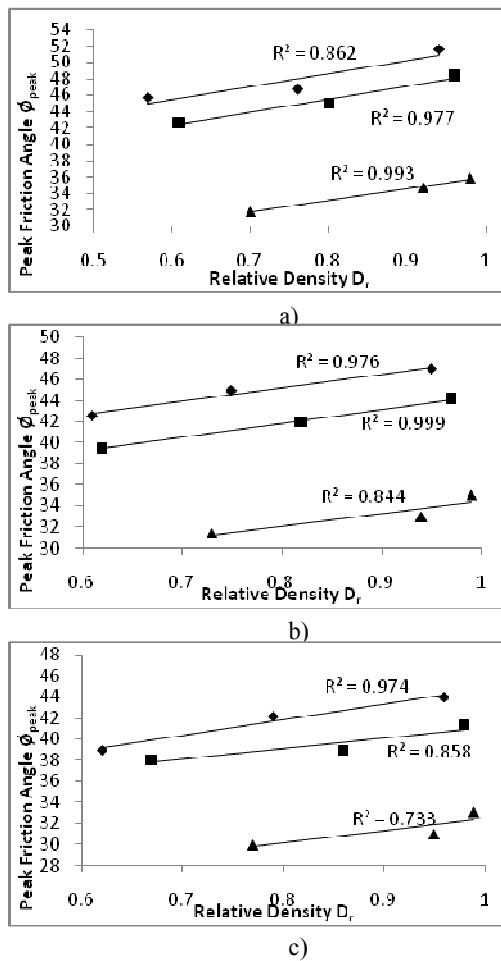


Figure 11: Peak friction angle versus relative density of all the samples with (a) 25kPa, (b) 50kPa (c) 100kPa normal stress (σ_n).

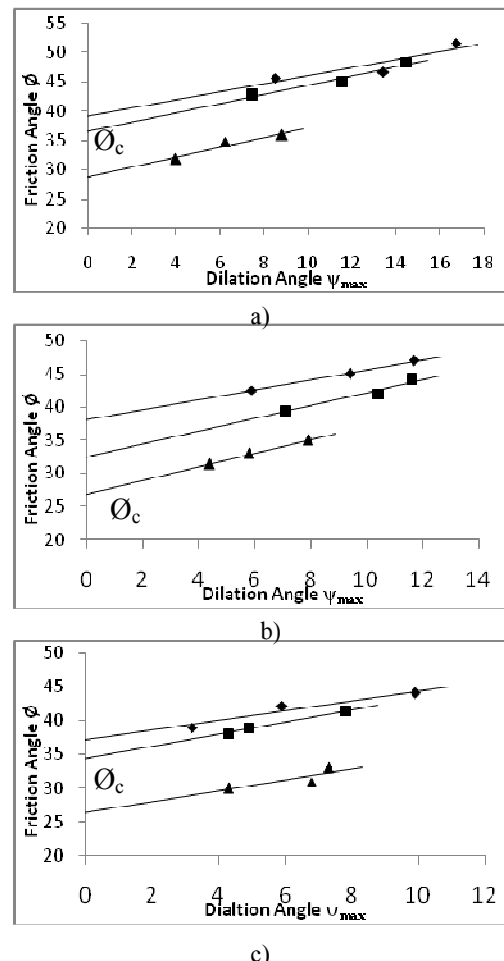


Figure 12: The determination of critical friction angle for all the samples under (a) 25kPa (b) 50kPa (c) 100kPa normal stress.

Table 4 summarises the equation that is obtained from the straight line graphs in Figure 11. It shows that the slope of the lines is similar at the same normal stress for

the samples. The slope then decreases as the normal stress decreases for each sample. This shows that high normal stresses decrease the peak friction angle abruptly at high

relative densities. Table 5 shows the critical friction angle at zero dilatancy angle obtained from Figure 12 and it is compared with the critical friction angle which is computed from residual stresses. Residual stresses are obtained at the end of the maximum displacement of the direct shear stress as shown in Figure 10(a). It can be seen that both the peak (ϕ_{peak}) and critical (ϕ_{cr}) friction angle decreases as the normal stress (σ_n) increases for all the sample of similar relative density (D_r).

The sedimentary characteristics of the shapes of sand particles also play a significant role in the shear strength of the soil and it is not entirely dependent on the mineral-to-mineral friction [5][15]. Figure 13 shows the relationship of the sphericity and roundness to the

theoretical friction angle (ϕ_{cr}). The shear strength values of $SPu_{(L.Buzzard)}$ and $SPu_{(Kahang)}$ of similar C_u to this study are compared so that particle size distribution does not influence the outcome of the results. The graph shows that the roundness and sphericity of the particles show a significant effect on the critical friction angle (ϕ_{cr}). The graph in Figure 13 shows a trend where the critical friction angle decreases as both the roundness and sphericity increases. This phenomenon was also reported by Carvarretta et al. [16], where particle shapes has significantly influence the shearing resistance rather than the surface roughness itself due to the arrangement of the particles during shearing.

Table 4: Summary of the equations from Figure 10.

Figure 10a	Equation	Slope
SW	$\phi_{cr} = 15.85Dr + 36$	15.85
SPu(Kahang)	$\phi_{cr} = 15.86Dr + 32.8$	15.86
SPu(L.Buzzard)	$\phi_{cr} = 14.25Dr + 21.8$	14.25
Figure 10b	Equation	Slope
SW	$\phi_{cr} = 12.74Dr + 35.1$	12.74
SPu(Kahang)	$\phi_{cr} = 13.11Dr + 31.3$	13.11
SPu(L.Buzzard)	$\phi_{cr} = 12.01Dr + 22.5$	12.01
Figure 10c	Equation	Slope
SW	$\phi_{cr} = 14.71Dr + 30.1$	14.71
SPu(Kahang)	$\phi_{cr} = 10.11Dr + 31$	10.11
SPu(L.Buzzard)	$\phi_{cr} = 11.17Dr + 21.3$	11.17

Table 5: Determination of the critical friction angle.

	Critical friction angle (ϕ_{cr}) at $\psi = 0$	Critical friction angle (ϕ_{cr}) at residual stress
$\sigma_n = 25kPa$		
SW	39.3	40.3
SPu(Kahang)	36.5	36.1
SPu(L.Buzzard)	28.8	29.1
$\sigma_n = 50kPa$		
SW	38.1	38.5
SPu(Kahang)	32.5	35.4
SPu(L.Buzzard)	27.0	28.2
$\sigma_n = 100kPa$		
SW	37.2	36.5
SPu(Kahang)	34.4	34.7
SPu(L.Buzzard)	26.4	26.7

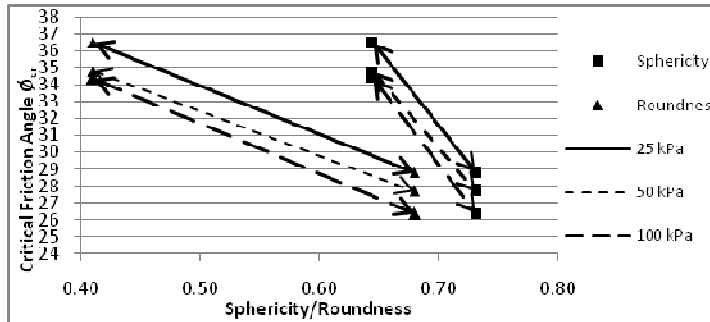


Figure 13: The relationship of the sphericity and roundness to the critical friction angle (ϕ_{cr}).

Occurrence of Dilatancy on the Sand Samples

When a soil is subjected to a normal stress, the particles in the soil tend to be more compacted and an interlocking structure would occur between the particles. This will restrict the freedom of the particles to move around one another, hence causing a bulk expansion in volume of the material when it is under shear deformation. This occurrence is called dilatancy.

However, the increase in effective normal stress will suppress the interlocking grains to expand in volume. Therefore, the ability of the dense assembly of the soil grains to expand depends on the magnitude of the normal effective stress (σ_n) [7]. The increase in shear strength with density is primarily due to the increased tendency of the sample to dilate and the work done in overcoming frictional forces [17].

Figure 14 shows the variation of maximum dilation angle (ψ) with different relative densities of Kahang sands and at different normal stresses. It can be seen that

SW with a higher uniformity coefficient has higher dilation angles compared to $SPu_{(Kahang)}$ with similar relative density (D_r) regardless of the different normal stresses (σ_n). It can also be seen that as the normal stress increases, the maximum dilation angle decreases. Figure 14(c) shows that there is not much of a difference in the dilation angle values of each sample at high normal stress of 100kPa. As stated, higher normal stress suppresses dilatancy. However, an increase in sphericity and roundness decreases the dilatancy (ψ). Figure 15 shows the $SPu_{(L.Buzzard)}$ has a higher mean sphericity and roundness values compared to $SPu_{(Kahang)}$ and it shows

lower dilatancy values. $SPu_{(Kahang)}$ tend to have higher dilation angles at low level normal stress (σ_n), but the values decrease as the normal stress increases up to a point where the values are the same as $SPu_{(L.Buzzard)}$. The increasing normal stresses have only little effect on the dilation angle of $SPu_{(L.Buzzard)}$. This can be explained as angular particles tend to be more interlocking and it obstructs the mobility of the particles, making it to expand in volume when shear displacement is induced. Smooth and rounder particles have the ease to move around each other, which explains its low dilation angles regardless of the normal stress.

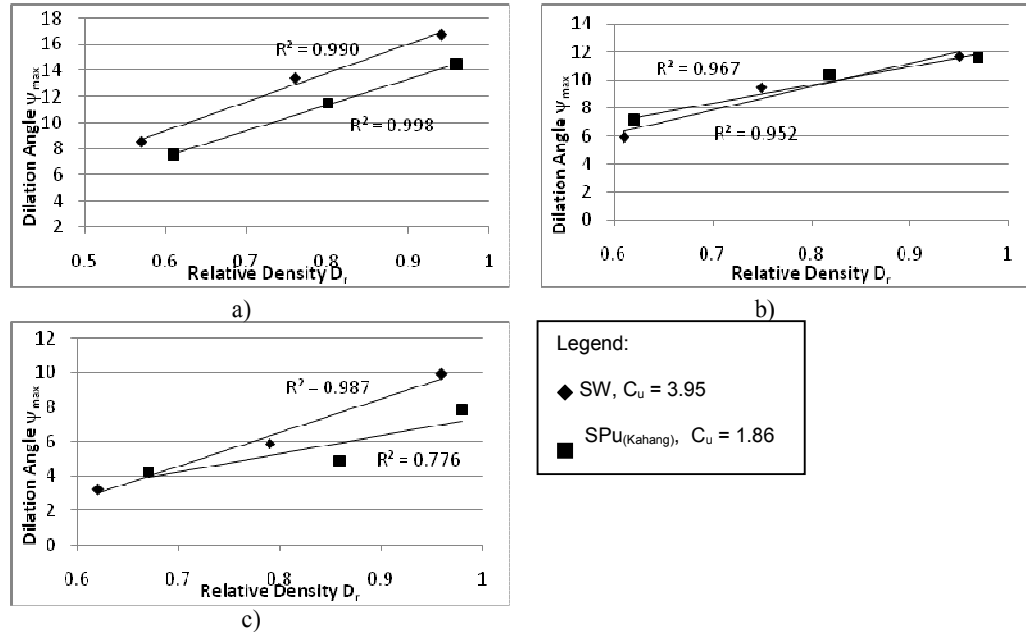


Figure 14: Dilation angle versus the relative density with (a) 25kPa, (b) 50kPa and (c) 100kPa normal stresses of sand with different uniformity coefficient (C_u).

The net effect of the dilatancy is that the failure envelope deviates from the usual straight line and is slightly curved (see Figure 16) for all test samples. This confirms equation 1 where the shear stress is dependent on the normal stress (σ_n) and angle of dilatancy (ψ). An increase in normal stress decreases dilatancy resulting in the decrease of shear strength (τ). Figure 16 compares the failure envelope of the sample with the lowest relative density and no dilatancy represented by a straight line from the origin. However, Hamidi et. al. [13], found that the curved envelop also happens due to particle crushing with high normal stress. As stated previously, particle crushing was avoided in this study. It can be seen that the difference in the failure envelop of dense and loose $SPu_{(L.Buzzard)}$ is not much. This is due to the low dilatancy angle on the soil even at low normal stress. In soil testing, it can be said that soil consolidated at low normal stress seems to increase the soil strength more than which is consolidated at a higher stress.

6. Conclusion

The sedimentological behaviour of sand particles has emerge to be a significant soil index property that needs to be looked further into. The systematic assessment of particle shapes and gradation characteristics will lead a better understanding of sand behaviour. Direct shear box testing on the sand samples has shown that gradation has a significant effect on the peak friction angles (ϕ_{peak}) and the critical friction angles (ϕ_{cr}). Both the uniformly graded sands $SPu_{(Kahang)}$ and $SPu_{(L.Buzzard)}$ shows lower (ϕ_{peak}). Comparing between the two, $SPu_{(L.Buzzard)}$ has higher sphericity and roundness values which gives a decrease in (ϕ_{peak}) of at least 6 degrees as compared to $SPu_{(Kahang)}$.

The shape characteristics of the coarse sand also have an influence in the occurrence of dilatancy. Higher sphericity and roundness values tend to have lower dilation angles as compared to the other soils. Dilation is also however dependent on the relative density and the normal stress (σ_n) has a significant effect on the shear

strength of the soil. Based on Budhu [7], the dilation angle increases as the normal stress decreases. This has caused the failure envelop to become curved for denser sand samples. Loose sand sample which exhibits zero dilatancy has shown a straight line failure envelope. The increasing normal stresses have only little effect on the dilation angle of SPU(L.Buzzard) as compare to SPU(Kahang). Angular particles tend to be more interlocking in its structure and obstructs the mobility of the particles during

shearing, resulting in the expansion of volume. Rounder particles however, have the ease to move and slide around each other, therefore it explains the low dilation angles regardless of the normal stress that is induced on it. As a result, the particle gradation and shapes of the coarse grained sands really needs to be understood in detail as it has a significant effect on the its shear strength and dilatancy.

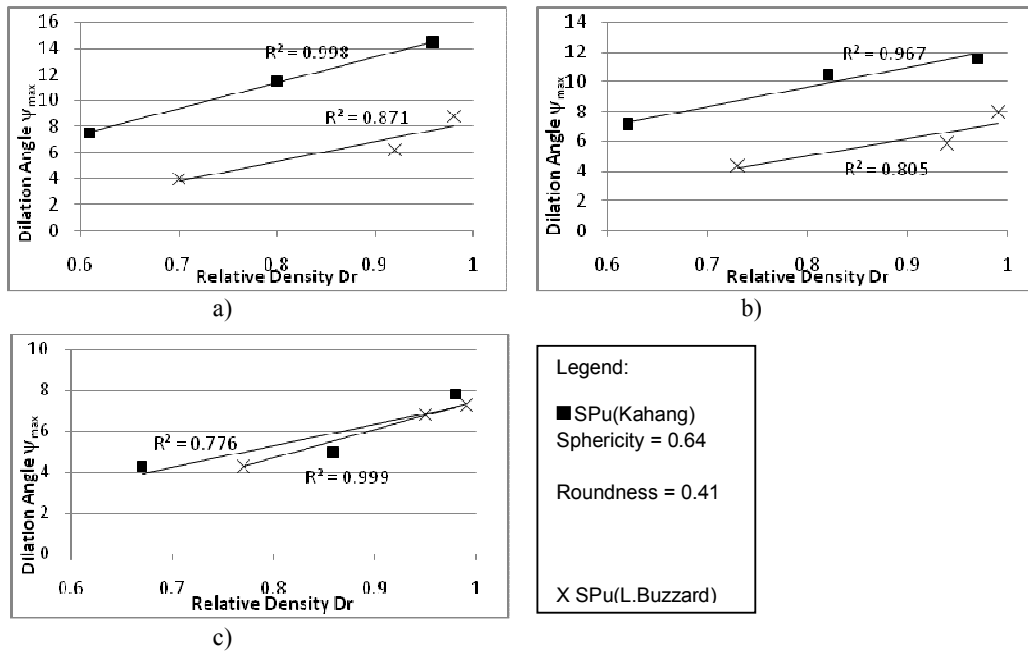


Figure 15: The effect of sphericity and roundness on the dilation angle with (a) 25kPa, (b) 50kPa and (c) 100kPa of normal stress (σ_n).

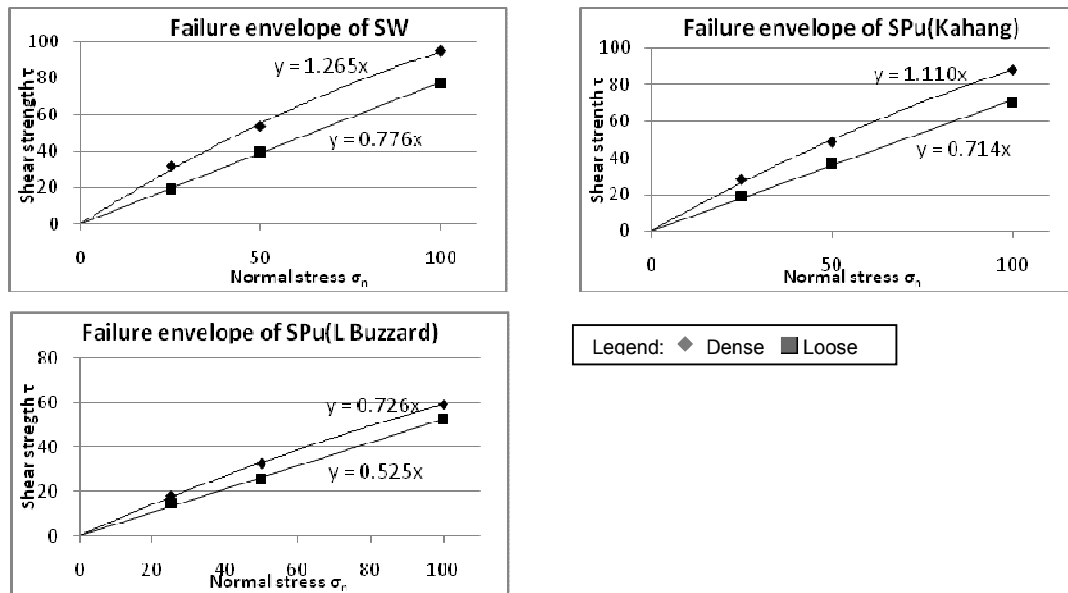


Figure 16: Failure envelope of samples with different relative densities.

NOTATIONS

c	Cohesion
C_u	Uniformity coefficient
C_c	Coefficient of gradation
D_{10}	Diameter which 10% of the total soil mass is passing
D_{60}	Diameter which 60% of the total soil mass is passing
D_r	Relative Density
dx	Horizontal displacement
dv	Vertical displacement
e_{max}	Maximum void ratio
e_{min}	Minimum void ratio
ϕ	Friction angle
ϕ_{peak}	Peak friction angle
ϕ_{cr}	Critical friction angle
ψ	Dilatancy angle
σ_n	Normal stress
R	Roundness
S	Sphericity
τ	Shear strength
τ_{peak}	Peak shear stress
τ_r	Residual stress

ACKNOWLEDGEMENT

The author would like to acknowledge the Research Center for Soft Soil (RECESS) laboratory, the laboratory staff and the guidance of the supervisory team.

REFERENCES

- [1] Harris, P.M., Thurrell, R.G., Healing, R.A. & Archer, A.A. (1974). Aggregates in Britain. Proc. R. Soc/ London, A339, 329-253.
- [2] Archer, A.A., (1972). Sand and gravel as aggregate. Miner. Dossier Miner. Resour. Consult. Comm. No. 4. H.M.S.O.
- [3] Burningham H. & French J.R., (2007). Morphodynamics and sedimentology of mixed-sediment inlets. Journal of Coastal Research, SI 50, pg 710 – 715.
- [4] Belkhatir, M., Arab, A., Della, N., Missoum, H. & Schanz, T. (2010) Effect of grading characteristics on the undrained shear strength of sand-silt mixture: International Symposium on Seismic Construction Zone Hassiba Benbouali University of Chlef (Algeria), 26 to 27 October 2010.
- [5] Cho, G.C, Dodds, J. & Santamarina, J.C. (2006). Particle shape effects on packing density, stiffness and strength: Natural and crushed sands. Journal of Geotechnical and Geoenvironmental Engineering, ASCE, Vol. 132, No 5.
- [6] Tsomokos A. & Georgiannou V.N. (2010), "Effect of grain shae and angularity on the undrained response of fine sands". Canadian Geotechnical Journal, Vol. 47, Number 5.pg 539 to 551.
- [7] Budhu, M. (2000). Soil mechanics and foundations: John Wiley & Sons, New York
- [8] British Standard Institution (BSI). BS 1377: British Standard Method of Test for Soils for Civil Engineering Purposes.
- [9] Head, K.H. (1992). Manual of soil laboratory testing. Vol 1: Soil classification and compaction test. Pentech Press, London.
- [10] Bolton, M.D. (1986). "The strength and dilatancy of sands" Géotechnique., 36(1), 65-78.
- [11] Bolton, M.D. (1987). "The strength and dilatancy of sands" Discussion. Géotechnique., 37(1), 219-226.
- [12] Whitlow,R. (2001), Basic Soil Mechanics, Prentice Hall, Harlow
- [13] Hamidi, A. Alizadeh, M. & Soleimani, S.M. (2009). Effect of particle crushing on shear strength and dilation characteristics of sand-gravel mixtures: International Journal of Civil Engineering. Vol. 7, No. 1, March 2009.
- [14] Simoni, A. & Houlsby, G.T. (2006). The direct shear strength and dilatancy on sand-gravel mixtures. Geotechnical and Geological Engineering. Vol 24, 523-549
- [15] Chan, L. C. Y., & Page, N. W. (1997). "Particle fractal and load effects on internal friction in powders" Powder Technol., 90, 256-266.
- [16] Cavarretta, I, Coop, M. & Sullivan C.O. (2010). The Influence of Particle Characteristics on the Behaviour of Coarse Grained Soils. Geotechnique 60, No. 6, pg 413 – 423.
- [17] Wijeyesekera, D.C., Hachouf, K. and Warnakulasuriya, S. (1998) "The significance of dilatancy of the backfill on the soil structure interaction pf polypropylene reinforcement", Proceedings of the 2nd international Conference on ground improvement techniques, pg 537-544, Singapore.